



Original articles

Research article

<https://doi.org/10.17308/kcmf.2024.26/11940>

The influence of benzoic acid moisture on the proton exchange process in lithium niobate crystals

I. V. Petukhov[✉], V. I. Kichigin, A. R. Kornilitsyn, A. S. Yakimov

Perm State University,
15 ul. Bukireva, Perm 614990, Russian Federation

Abstract

The purpose of this study was the investigation of the influence of water impurities in benzoic acid, used as a source of protons during proton exchange on lithium niobate crystals, on the process of formation of proton exchange waveguides, their structure and phase composition.

To carry out the research, prism coupling method, X-ray diffraction analysis, IR absorption spectroscopy, and optical microscopy in polarized light were used. It was established that an increase in the moisture content in benzoic acid affected the optical characteristics of the waveguides and slightly increased the stress (strain) of the proton exchange layers. Subsequent annealing significantly equalized the characteristics of the waveguides.

When performing proton exchange, the moisture content of benzoic acid must be taken into account to obtain reproducible and stable performance of integrated optical devices with proton exchange waveguides.

Keywords: Lithium niobate, Proton exchange, Waveguide, Structure, Phase composition, Benzoic acid, Melt, Moisture

Funding: The study was funded by the Russian Foundation for Basic Research and the Perm Krai within the framework of scientific project No. 20-42-596001.

For citation: Petukhov I. V., Kichigin V. I., Kornilitsyn A. R., Yakimov A. S. The influence of benzoic acid moisture on the proton exchange process in lithium niobate crystals. *Condensed Matter and Interphases*. 2024;26(2): 295–303. <https://doi.org/10.17308/kcmf.2024.26/11940>

Для цитирования: Петухов И. В., Кичигин В. И., Корнилицын А. Р., Якимов А. С. Влияние влажности бензойной кислоты на процесс протонного обмена в кристаллах ниобата лития. *Конденсированные среды и межфазные границы*. 2024;25(2): 295–303. <https://doi.org/10.17308/kcmf.2024.26/11940>

✉ Igor V. Petukhov, e-mail: petukhov-309@yandex.ru

© Petukhov I. V., Kichigin V. I., Kornilitsyn A. R., Yakimov A. S., 2024



The content is available under Creative Commons Attribution 4.0 License.

1. Introduction

Proton exchange (PE) is one of the main modern technologies for producing optical waveguides in lithium niobate (LN) crystals for the manufacture of various integrated optical devices [1, 2]. The most widely used source of protons in PE is benzoic acid (BA) [3–5]. When LN is immersed into the molten BA part of the lithium ions in the surface layer of the LiNbO_3 crystal is substituted by hydrogen ions, and an $\text{H}_x\text{Li}_{1-x}\text{NbO}_3$ solid solution is formed. Proton penetration depth into LiNbO_3 depends on conditions, it ranges from fractions of a micron to several microns. As a result, the refractive index n_e of the surface (proton exchange) layer of the crystal increases [3, 6–9], which is a prerequisite for the appearance of the waveguide properties of this layer.

Immediately after proton exchange and subsequent annealing, depending on the value of normalized concentration x of protons, seven different $\text{H}_x\text{Li}_{1-x}\text{NbO}_3$ phases can form [3, 8]. The formation of α -phases ($x < 0.12$) during post-exchange annealing ensures the stable optical characteristics of waveguides and restoration of the electro-optical coefficient.

Despite the fact that PE is a widely used technological process, its individual aspects continue to be actively researched [10–12].

To obtain reproducible characteristics of waveguides, it is not enough to strictly control the duration of processing and annealing, as well as the temperature regime. The process of formation of optical waveguides is influenced by the chemical composition of lithium niobate [13]. In congruent lithium niobate, commonly used for integrated optical devices, the ratio $\text{Li}_2\text{O}:\text{Nb}_2\text{O}_5$ may vary among different manufacturers [13, 14], therefore the characteristics of the formed waveguides will also differ.

The proton exchange process is also affected by the presence of impurities in benzoic acid, including water impurities. The moisture content in BA varies among different manufacturers; the moisture content of BA is also affected by the conditions and duration of storage of benzoic acid. The influence of moisture impurities in BA on the PE process was noted in a number of studies [15–18].

It was previously shown that benzoic acid in melts is present predominantly in an

undissociated state in the form of dimers [19]. Moisture impurities increase the electrical conductivity of benzoic acid melts, promote its dissociation and somewhat accelerate proton exchange [20].

This study is a continuation of a previously conducted research into the electrical conductivity of benzoic acid melts with a controlled content of moisture impurities [20]. The goal of the study was to establish the influence of controlled moisture content in BA on the process of proton exchange, the phase composition of proton exchange layers and the optical characteristics of PE waveguides.

2. Experimental

To evaluate the effect of moisture impurities on the PE process, several samples of benzoic acid were used: 1) benzoic acid, analytical grade as-received (hereinafter this sample is called unprocessed BA (NBA)); 2) BA after drying in a desiccator over anhydrous calcium chloride for 7 days (DBA); 3) BA after exposure to conditions of relative humidity of air of 100% for 5–7 days (WBA). When dried over anhydrous CaCl_2 the BA weight decreased by approximately 0.02%; when exposed to conditions of 100% moisture, the BA weight increased by ~0.02%.

For the study, samples of congruent lithium niobate (X-cut) produced by CQT (PRC) with the size of 15x10x1 mm were used. Proton exchange was carried out in a melt of benzoic acid at a temperature of 175 °C for 6 h, which led to the formation of a multi-mode waveguide. After PE, the reactor with the samples was removed from the furnace to cool to room temperature. Post-exchange annealing was carried out in an air atmosphere at 370 °C.

For the obtained planar waveguides, the depth profiles of the extraordinary refractive index $n_e(x)$ were determined by the prism coupling method using the inverse Wentzel–Kramers–Brillouin method [21] and $\Delta n_e(0)$ values at the surface of the waveguide at wavelength $\lambda = 0.633 \mu\text{m}$ were determined.

For the detection of changes on the surface of the proton-exchanged layer of the LN crystal caused by phase transformations, the optical microscopy in polarized light (Olympus BX 51) was used.

X-ray diffraction studies of lithium niobate samples were carried out using DRON-UM1 double crystal diffractometer in Co-anode radiation (wavelength $\lambda_{\beta} = 1.62073 \text{ \AA}$). The $\theta/2\theta$ -curves were registered and used for the determination of ε_{33} strain in the direction of the normal to the surface according to Bragg equation:

$$\varepsilon_{33} = \Delta d/d = -\Delta\theta \operatorname{ctg} \theta,$$

where Δd is change in interplanar spacing d , $\Delta\theta$ is the angular distance between the diffraction reflection maxima from the lithium niobate substrate and from the corresponding PE phase, θ – Bragg reflection angle.

Lithium niobate samples after PE were also studied using IR absorption spectroscopy on a Hewlett Packard Spectrum Two spectrophotometer in the range $400\text{--}6000 \text{ cm}^{-1}$.

3. Results and discussion

The refractive index profile of the waveguides after PE has a stepwise character (Fig. 1). In all three cases, the $\Delta n_e(0)$ had similar values, which probably indicated a qualitatively identical phase composition of the uppermost layer of the proton-exchanged region. The depth of the waveguide layer obtained in the WBA was noticeably higher than for the other two BA samples. This indicated a more intense PE in the presence of water impurities.

In the IR spectra of the samples after proton exchange (Fig. 2), the following pattern can be noted: a wide peak at $3200\text{--}3400 \text{ cm}^{-1}$, corresponding to interstitial protons (presumably the β_2 -phase), was the most intense for the proton exchange layers obtained in the WBA, and in the DBA the peak intensity was the lowest. The same is true for the narrow peak corresponding to absorption at 3500 cm^{-1} . Measurements of IR spectra indicated a natural increase in the concentration of protons in the PE layer on lithium niobate with an increase in the moisture content in benzoic acid used for PE.

After PE, regardless of the amount of impurity water in the BA, two peaks were recorded on the $\theta/2\theta$ -curves (Fig. 3). It should be noted that after PE in the melt of dried benzoic acid, the intensity of these peaks was maximum. Decomposition of the obtained curves allowed to identify a larger number of peaks corresponding to different proton-exchange phases (Table 1).

The lithium niobate peak had a shoulder on the right, due to the presence of the α -phase, formed at the PE-layer/ LiNbO_3 interface and characterized by the lowest proton concentration [3]. There were three phases in the proton exchange layers (the β_1 -, β_2 -phases and probably the κ_2 -phase). With the increasing ordinal number of the β -phase, the concentration of protons increased [3]. The phase with a higher proton concentration was located closer to the

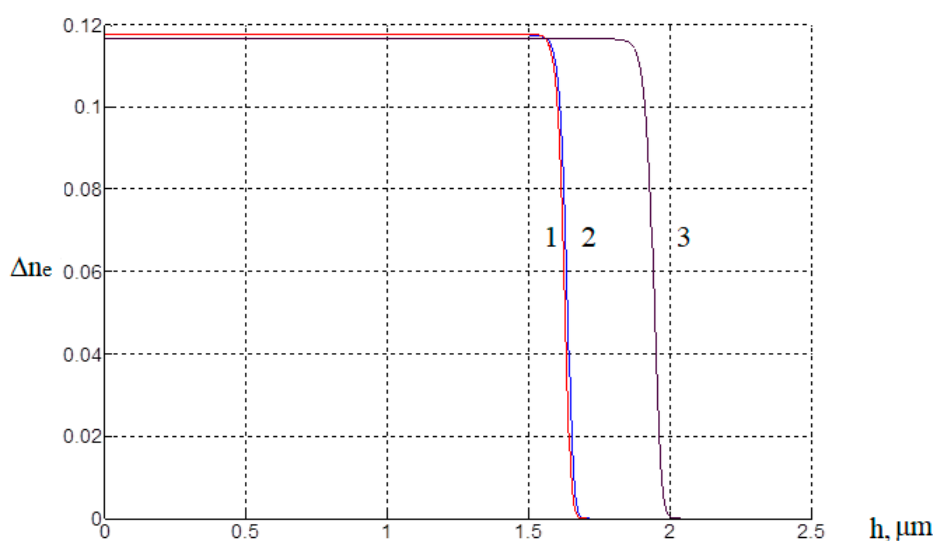


Fig. 1. Refractive index profiles in proton-exchanged waveguides, PE $175 \text{ }^\circ\text{C}$, 6 h in different samples of benzoic acid: 1 – DBA, 2 – NBA, 3 – WBA

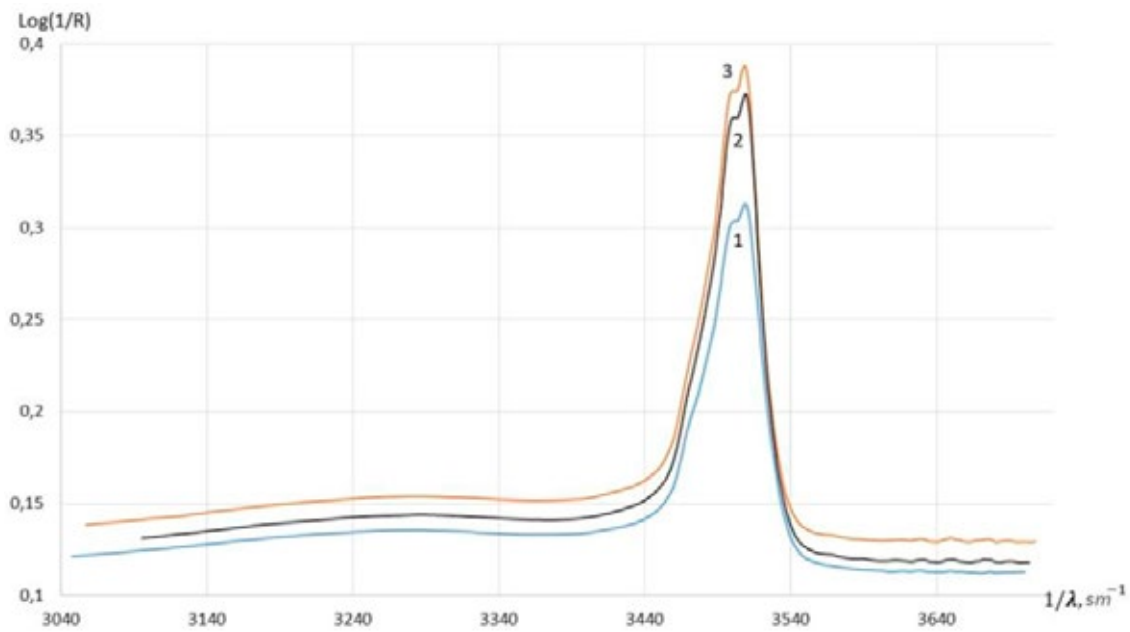


Fig. 2. IR absorption spectra of lithium niobate after PE 175 °C, 6 h: 1 – DBA, 2 – NBA, 3 – WBA

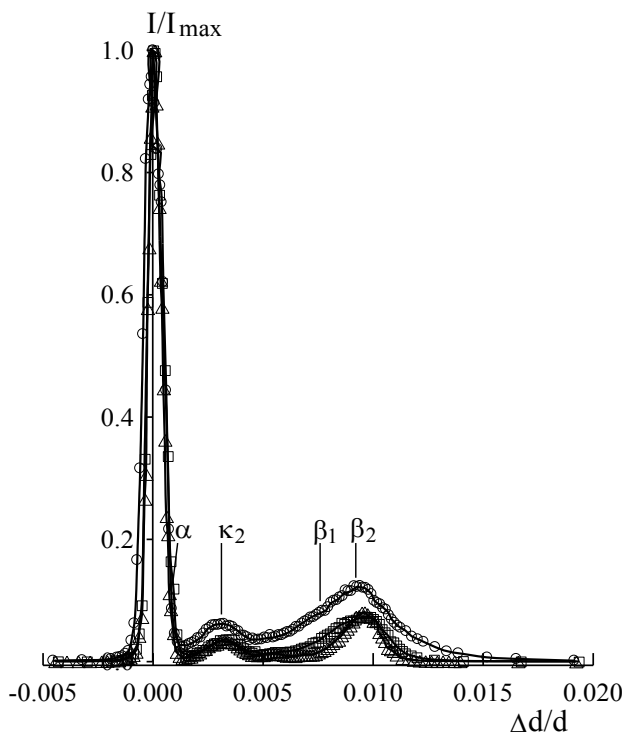


Fig. 3. $\theta/2\theta$ curves for proton-exchanged layers on lithium niobate after PE 175 °C, 6 h. (○) in DBA, (Δ) in NBA, (□) in WBA. Reflection from (110) planes

crystal surface [3, 22]. Although, according to the authors of [3], the formation of the κ_2 -phase is possible only as a result of annealing, according to the results of [23], the κ_2 -phase, probably, can form immediately after PE (in the 175 °C, 6 h mode).

As the moisture content in BA increased, the proportion of the β_1 -phase also increased, and increase in the strains of the most stressed β_2 -phase was observed. In [3, 8] it was stated that the β_1 -phase is the most stressed on the X-cut of LiNbO_3 (under PE conditions at 240 °C). However, the results of a study [23], in which a gradual etching of the PE layer obtained at 175 °C was performed, indicated that the etching off a β_2 -phase located on the surface decreased the intensity of the peak with the highest strain values.

The decrease in the intensity of the peaks corresponding to proton-exchange phases with increasing moisture content in the BA was possibly due to higher stresses and higher structure imperfection of these phases. A similar ratio of intensities of proton-exchange phases occurred when comparing the $\theta/2\theta$ -curves of lithium niobate without treatment and with pre-treatment of the crystal surface with Ar plasma before proton exchange [24]. Plasma treatment significantly increased the structure imperfection of a thin surface layer of lithium niobate, led to an increase in strain in proton-exchange phases and a decrease in the intensity of the corresponding peaks on the $\theta/2\theta$ -curves. The results obtained may indicate an intensification of proton exchange as the content of water impurities in benzoic acid increases.

Table 1. Decomposition of the peaks in $\theta/2\theta$ curves for proton-exchanged layers obtained in different samples of benzoic acid

Benzoic acid	Peak (phase)	Relative peak intensity	$\epsilon_{33} \cdot 10^3$	Full width at half maximum $\cdot 10^5$	Relative peak area, %
DBA	1(LN)	0.95	0	0.74	42.7
	2(α)	0.48	0.42	0.51	14.8
	3(κ_2)	0.058	3.10	3.06	10.7
	4(β_1)	0.022	6.05	2.00	2.7
	5(β_2)	0.12	9.21	4.09	29.1
HBK	1(LN)	0.82	0	0.51	43.6
	2(α)	0.45	0.33	0.57	26.5
	3(κ_2)	0.022	3.20	1.34	3.0
	4(β_1)	0.012	4.10	9.96	12.8
	5(β_2)	0.073	9.49	1.86	14.1
WB	1(LN)	0.91	0	0.61	49.8
	2(α)	0.37	0.47	0.64	21.4
	3(κ_2)	0.033	3.18	2.32	6.9
	4(β_1)	0.029	7.98	3.93	10.3
	5(β_2)	0.058	9.86	2.24	11.7

An increase in the benzoic acid moisture led to an increase in the concentration of protons in the PE layer. This can explain the slower decrease in the refractive index (Fig. 4) for samples obtained in the WBA during annealing at the initial stage. The observed changes correspond to the literature data [15, 16].

Annealing for 2 h changed the phase composition of the PE layers (Fig. 5, Table 2). The results of decomposition of $\theta/2\theta$ -curves obtained

for two orders of reflection are shown in Table 2. The presence of the κ_1 -phase was more clearly visible on the $\theta/2\theta$ -curves of the second order of reflection (Fig. 5b).

During annealing the β -phases located at the surface of the PE layer turned into the κ_2 - and κ_1 -phases; the presence of the κ_1 -phase was confirmed by micrographs of the surface of protonated layers (Fig. 6). The resulting modulated structures represented the formations

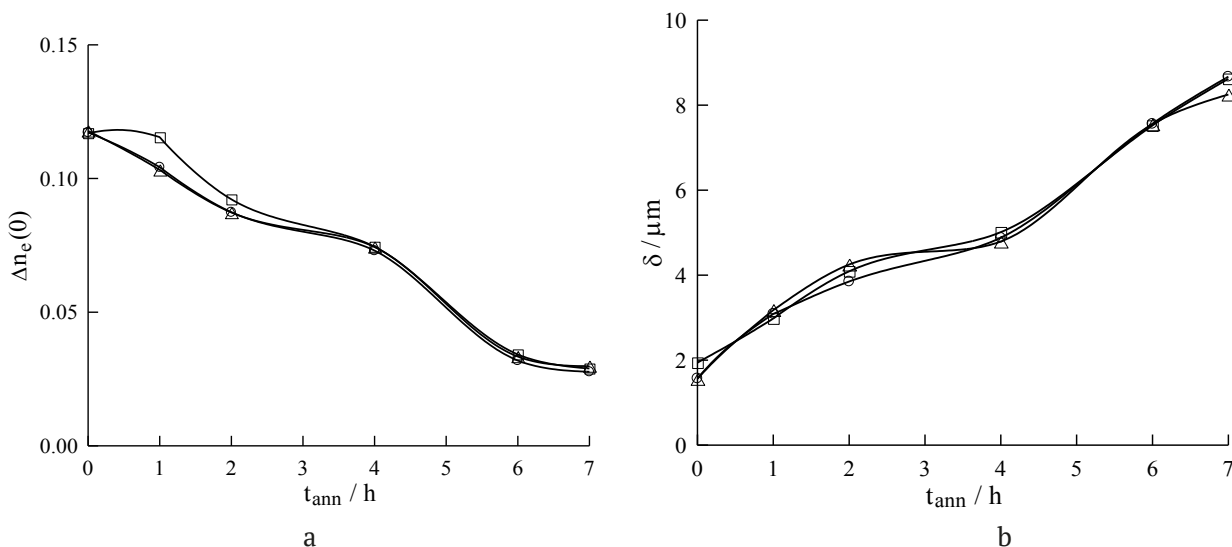
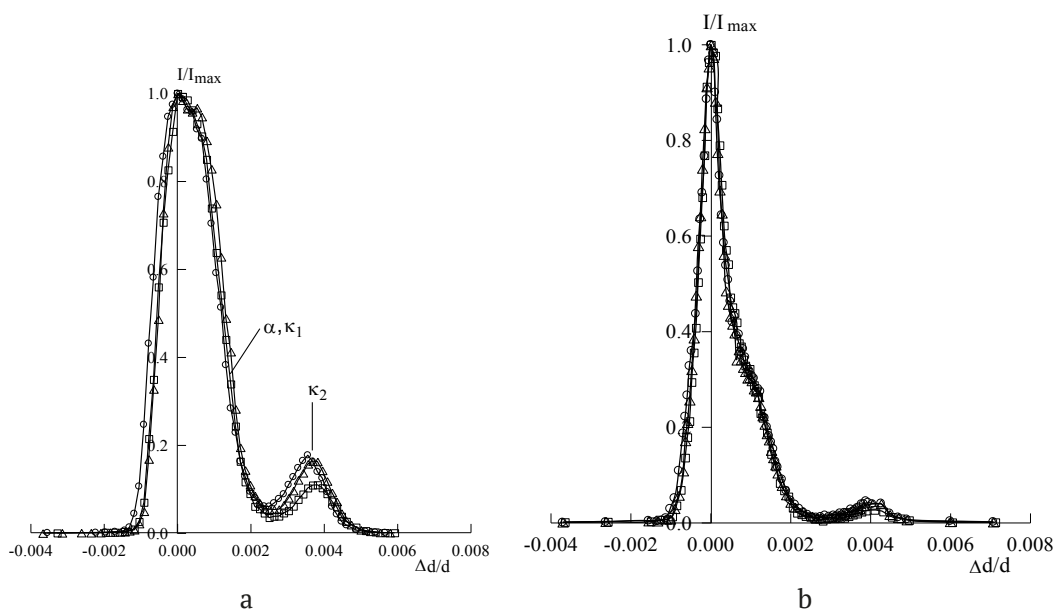

Fig. 4. $\Delta n_e(0)$ (a) and waveguide depth (b) as functions of annealing duration. (○) PE in DBA, (△) PE in NBA, (□) PE in WBA

Table 2. Decomposition of the peaks in $\theta/2\theta$ curves for proton-exchanged layers obtained in different samples of benzoic acid, after annealing 370 °C, 2 h

Benzoic acid	Peak (phase)	Relative peak intensity	$\epsilon_{33} \cdot 10^3$	Full width at half maximum $\cdot 10^5$	Relative peak area, %
Reflection from (110) planes					
DBA	1 (LN)	0.93	0	0.58	52.1
	2 (α)	0.48	0.83	0.44	20.1
	3 (κ_1)	0.31	1.32	0.59	17.8
	4 (κ_2)	0.17	3.53	0.60	10.0
NBA	1 (LN)	0.87	0	0.42	37.4
	2 (α)	0.54	0.44	0.43	23.8
	3 (κ_1)	0.48	0.93	0.60	28.7
	4 (κ_2)	0.16	3.67	0.62	10.1
WBA	1 (LN)	0.83	0	0.47	42.4
	2 (α)	0.55	0.74	0.48	28.0
	3 (κ_1)	0.31	1.21	0.66	22.0
	4 (κ_2)	0.11	3.85	0.63	7.5
Reflection from (220) planes					
DBA	1 (LN)	0.97	0	0.33	60.0
	2 (α)	0.24	0.67	0.30	13.7
	3 (κ_1)	0.23	1.20	0.50	21.7
	4 (κ_2)	0.04	3.97	0.61	4.7
NBA	1 (LN)	0.96	0	0.36	65.9
	2 (α)	0.16	0.69	0.23	7.0
	3 (κ_1)	0.26	1.13	0.46	22.6
	4 (κ_2)	0.04	3.95	0.65	4.5
WBA	1 (LN)	0.99	0	0.36	67.4
	2 (α)	0.19	0.67	0.23	8.2
	3 (κ_1)	0.25	1.13	0.45	21.4
	4 (κ_2)	0.03	4.03	0.58	2.9


Fig. 5. $\theta/2\theta$ curves for proton-exchanged layers on lithium niobate after PE 175 °C, 6 h and annealing 370°C, 2 h. (○) PE in DBA, (△) PE in NBA, (□) PE in WBA. Reflection from the planes: a – (110), b – (220)

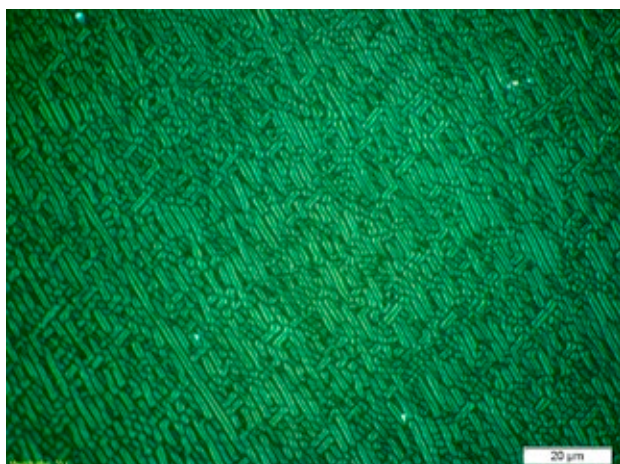


Fig. 6. Micrograph of lithium niobate sample after proton exchange (175 °C, 6 h) and annealing (370 °C, 2 h)

of κ_1 -phase as a result of relaxation of high internal stresses in proton-exchange layers [25]. Phase κ_2 , which was formed during PE under the β -phases, upon annealing was transformed into the κ_1 and α phases.

An analysis of the results shown in Table 2 indicated an increase in ϵ_{33} values, corresponding to the κ_2 -phase, with increasing content of moisture impurities in benzoic acid. It also follows from the decomposition of reflections from (110) planes that an increase in moisture content increased the total intensity of proton-exchange phases (κ_2 -, κ_1 - and α -phases). In the case of reflection from the (220) planes, which contain information about the structure of deeper layers, an increase in the moisture of the BA led to an increase in the intensity of reflections from lithium niobate, while the total intensity from the κ_2 - and κ_1 -phases changed slightly.

As the annealing duration increased, the differences in the characteristics of the waveguides obtained in the DBA, NBA, and WBA decreased (Fig. 4). The Δn_e value is determined by the phase composition and concentration of protons in the PE layer. For each phase the dependence of Δn_e from normalized x concentration in $H_xLi_{1-x}NbO_3$ is different. The strongest dependence of $\Delta n_e(0)$ on x was observed at average x values (about 0.4), and at high x and especially at low x the dependence was weak [4]. Upon annealing > 4 h, the transition to the α -phase (low x) begins, and the dependence of $\Delta n_e(0)$ on x significantly weakened. The maximum difference $\Delta n_e(0)$ for

DBA and WBA was observed at an annealing time of 1–2 h (Fig. 4a), when the main phases were κ_2 - and κ_1 -phases ($x = 0.12$ – 0.44 [26]), for which $d\Delta n_e(0)/dx$ had the highest values. The reduction of differences in the depth δ of waveguides with an annealing time of more than 4 h (Fig. 4b) can be explained by the fact that the effective proton diffusion coefficient D_H in the PE layer on lithium niobate depends on x . In the α -phase region this dependence was quite strong, and with increase in x the D_H magnitude in X-cut crystals decreased [27]. Since the hydrogen concentration in the PE layer obtained in the WBA was higher, the diffusion coefficient in it was lower and weakened the possible increase of δ due to the higher x in the layer adjacent to the surface of the crystal.

Thus, the presence of small amounts of water in BA accelerates proton exchange. This may be due to the fact that water impurities in the benzoic acid melt promote both the transition of BA dimers into monomers and the dissociation of benzoic acid. This indicates an increase in the electrical conductivity of benzoic acid melts with increasing impurity water content [20]. The relatively small effects were due to the low concentration of water, even in the acid with the highest moisture content there was one molecule of water per about 300 molecules of benzoic acid. However, to obtain reproducible optical characteristics of integrated optical devices that use proton exchange, the moisture content of the benzoic acid used for proton exchange must be controlled.

4. Conclusions

The presence of moisture in benzoic acid used for proton exchange on lithium niobate crystals, affects the optical characteristics of waveguides and slightly increases the stress (strain) of the proton exchange layers. Subsequent annealing significantly equalizes the characteristics of the waveguides.

When performing proton exchange, the moisture content of benzoic acid must be taken into account to obtain reproducible and stable performance of integrated optical devices with proton exchange waveguides.

Contribution of the authors

The authors contributed equally to this article.

Conflict of interests

The authors declare that they have no known competing financial interests or personal relationships that could have influenced the work reported in this paper.

References

- Korkishko Yu. N., Fedorov V. A., Kostritskii S. M., ... Laurell F. Proton exchanged LiNbO₃ and LiTaO₃ optical waveguides and integrated optic devices. *Microelectronic Engineering*. 2003;69: 228–236. [https://doi.org/10.1016/S0167-9317\(03\)00302-2](https://doi.org/10.1016/S0167-9317(03)00302-2)
- Kuneva M. Optical waveguides obtained via proton exchange technology in LiNbO₃ and LiTaO₃ – a short review. *International Journal of Scientific Research in Science and Technology*. 2016;2(6): 40–50.
- Korkishko Yu. N., Fedorov V. A. Structural phase diagram of proton-exchange H_xLi_{1-x}NbO₃ waveguides in lithium niobate crystals. *Crystallography Reports*. 1999;44(2): 237–246. Available at: <https://elibrary.ru/item.asp?id=13324513>
- de Almeida J. M. M. Design methodology of annealed H⁺ waveguides in ferroelectric LiNbO₃. *Optical Engineering*. 2007;46(6): 064601. <https://doi.org/10.1117/1.2744364>
- Cai L., Wang Y., Hu H. Low-loss waveguides in a single-crystal lithium niobate thin film. *Optics Letters*. 2015;40(13): 3013–3016. <https://doi.org/10.1364/OL.40.003013>
- Suchoski P. G., Findakly T. K., Leonberger F. J. Stable low-loss proton-exchanged LiNbO₃ waveguide devices with no electro-optic degradation. *Optics Letters*. 1988;13(11): 1050–1052. <https://doi.org/10.1364/OL.13.001050>
- Korkishko Y. N., Fedorov V. A., Feoktistova O. Y. LiNbO₃ optical waveguide fabrication by high-temperature proton exchange. *Journal of Lightwave Technology*. 2000;18(4): 562–568. <https://doi.org/10.1109/50.838131>
- Korkishko Yu. N., Fedorov V. A. Structural phase diagram of H_xLi_{1-x}NbO₃ waveguides: the correlation between optical and structural properties. *IEEE Journal of Selected Topics in Quantum Electronics*. 1996;2(2): 187–196. <https://doi.org/10.1109/2944.577359>
- Bazzan M., Sada C. Optial waveguides in lithium niobate: Recent developments and applications. *Applied Physics Reviews*. 2015;2(4): 040603. <https://doi.org/10.1063/1.4931601>
- Dörrer L., Tüchel P., Hüger E., Heller R., Schmidt H. Hydrogen diffusion in proton-exchanged lithium niobate single crystals. *Journal of Applied Physics*. 2021;129: 135105. <https://doi.org/10.1063/5.0047606>
- Dörrer L., Tüchel P., Uxa D., Schmidt H. Lithium tracer diffusion in proton-exchanged lithium niobate. *Solid State Ionics*. 2021;365: 115657. <https://doi.org/10.1016/j.ssi.2021.115657>
- Demin V. A., Petukhov M. I., Ponomarev R. S., Kuneva M. Dynamics of the proton exchange process in benzoic acid interacting with lithium niobate crystals. *Langmuir*. 2023;39(31): 10855–10862. <https://doi.org/10.1021/acs.langmuir.3c00957>
- Kostritskii S. M., Korkishko Y. N., Fedorov V. A., ... Aillerie M. Phase composition of channel proton-exchanged waveguides in different near-congruent LiNbO₃. *Ferroelectrics Letters Section*. 2020;47(1–3): 9–15. <https://doi.org/10.1080/07315171.2020.1799627>
- Volk T., Wöhlecke M. *Lithium niobate: defects, photorefraction and ferroelectric switching*. Berlin: Springer, 2008. 249 p. <https://doi.org/10.1007/978-3-540-70766-0>
- Petukhov I. V., Kichigin V. I., Mushinskii S. S., Minkin A. M., Shevtsov D. I. Effect of water contained in benzoic acid on the proton exchange process, the structure and the properties of proton-exchange waveguides in lithium niobate single crystals. *Condensed Matter and Interphases*. 2012;14(1): 119–123. (In Russ., abstract in Eng.). Available at: <https://elibrary.ru/item.asp?id=17711946>
- Mushinsky S. S., Minkin A. M., Kichigin V. I., ... Shur V. Ya. Water effect on proton exchange of X-cut lithium niobate in the melt of benzoic acid. *Ferroelectrics*. 2015;476(1): 84–93. <https://doi.org/10.1080/00150193.2015.998530>
- Rambu A. P., Apetrei A. M., Doutre F., Tronche H., De Micheli M. P., Tascu S. Analysis of high-index contrast lithium niobate waveguides fabricated by high vacuum proton exchange. *Journal of Lightwave Technology*. 2018;36(13): 2675–2684. <https://doi.org/10.1109/JLT.2018.2822317>
- Rambu A. P., Apetrei A. M., Tascu S. Role of the high vacuum in the precise control of index contrasts and index profiles of LiNbO₃ waveguides fabricated by high vacuum proton exchange. *Optics and Laser Technology*. 2019;118: 109–114. <https://doi.org/10.1109/JLT.2018.2822317>
- Kichigin V. I., Petukhov I. V., Mushinskii S. S., Karmanov V. I., Shevtsov D. I. Electrical conductivity and IR spectra of molten benzoic acid. *Russian Journal of Applied Chemistry*. 2011;84(12): 2060–2064. <https://doi.org/10.1134/S1070427211120081>
- Kichigin V. I., Petukhov I. V., Kornilitsyn A. R., Mushinsky S. S. Influence of humidity of benzoic acid on the electrical conductivity of its melts. *Condensed Matter and Interphases*. 2022;24(3): 315–320. <https://doi.org/10.17308/kcmf.2022.24/9853>
- Kolosovskii E. A., Petrov D. V., Tsarev A. V. Numerical method for the reconstruction of the refractive index profile of diffused waveguides. *Soviet Journal of Quantum Electronics*. 1981;11(12):

1560–1566. <https://doi.org/10.1070/QE1981v-011n12ABEH008650>

22. Kuneva M. Surface phase detection of proton-exchanged layers in LiNbO_3 and LiTaO_3 by IR reflection spectroscopy. *Bulgarian Chemical Communications*. 2013;45(4): 474–478.

23. Azanova I. S., Shevtsov D. I., Zhundrikov A. V., Kichigin V. I., Petukhov I. V., Volyntsev A. B. Chemical etching technique for investigations of a structure of annealed and un-annealed proton exchange channel LiNbO_3 waveguides. *Ferroelectrics*. 2008;374(1): 110–121. <https://doi.org/10.1080/00150190802427234>

24. Mushinsky S. S., Petukhov I. V., Kichigin V. I., Sidorov D. I., Semenova O. R., Ponomarev R. S. Influence of the pretreatment of lithium niobate surface with plasma and ultraviolet radiation on the proton exchange in benzoic acid melts. *IEEE 22nd International Conference of Young Professionals in Electron Devices and Materials (EDM)*. 2021;283–286. <https://doi.org/10.1109/EDM52169.2021.9507647>

25. Mushinsky S. S., Kichigin V. I., Petukhov I. V., Permyakova M. A., Shevtsov D. I. Structural phase transformations of proton-exchanged layers of lithium niobate during annealing. *Ferroelectrics*. 2017;508(1): 40–48. <https://doi.org/10.1080/00150193.2017.1286702>

26. Korkishko Yu. N., Fedorov V. A. Composition of different crystal phases in proton exchanged waveguides in LiNbO_3 . In: Wong K. K. (Ed.), *Properties of Lithium Niobate*. Chapter 3.2. London: INSPEC, The Institution of Electrical Engineers; 2002. p. 50–54.

27. Ito K., Kawamoto K. The dependence of the diffusion coefficient on the proton concentration in the proton exchange of LiNbO_3 . *Japanese Journal of Applied Physics*. 1997;36(11): 6775–6780. <https://doi.org/10.1143/JJAP.36.6775>

Information about the authors

Igor V. Petukhov, Cand. Sci. (Chem.), Associate Professor at the Department of Physical Chemistry, Perm State University, (Perm, Russian Federation).

<https://orcid.org/0000-0002-3110-668x>
petukhov-309@yandex.ru

Vladimir I. Kichigin, Cand. Sci. (Chem.), Research Fellow, Research Fellow at the Department of Physical Chemistry, Perm State University (Perm, Russian Federation).

<https://orcid.org/0000-0002-4668-0756>
kichigin@psu.ru

Andrey R. Kornilitsyn, Engineer, Photonics Laboratory, Perm State University (Perm, Russian Federation).

<https://orcid.org/0000-0002-8267-0168>

Aleksandr S. Yakimov, Student, Faculty of Chemistry, Perm State University (Perm, Russian Federation).

fantom.500@mail.ru

Received 10.08.2023; approved after reviewing 07.09.2023; accepted for publication 16.10.2023; published online 25.06.2024.

Translated by Valentina Mittova